

Activation of dioxygen molecules on dinuclear metal centers

YOSHIHIKO MORO-OKA

Research Laboratory of Resources Utilization, Tokyo Institute of Technology,
4259 Nagatsuta Midori-ku, Yokohama 226-8503, Japan

Abstract. Activation of dioxygen molecules on transition metal centers, especially dinuclear metal centers was systematically investigated using hydrotris(3,5-dialkylpyrazolyl)borate ligands from both organometallic and bioinorganic viewpoints. Physicochemical data and X-ray crystallography of synthesized dicopper-O₂ complexes revealed a $\mu\text{-}\eta^2\text{:}\eta^2$ coordination mode which was proposed as the most probable model of *oxyhemocyanin*. Dioxygen species bound to dinuclear cobalt and nickel centers are quite active and react rapidly with C–H groups in ligands giving oxygenated products even at room temperature. The stability of $(\mu\text{-}\eta^2\text{:}\eta^2\text{-O}_2)\text{M}_2$ complexes depends on the electron-donating ability of the central metal atoms and the difference arises mainly from the extent of back donation to the antibonding O–O orbital.

Keywords. Dioxygen molecule; catalytic oxidative reactions; cobalt peroxo complexes; transition metal species.

1. Introduction

Oxidation and oxygenation with dioxygen molecule are involved in important biological processes such as metabolism and energy production, and many processes are associated with metalloproteins, a group of proteins which involve transition metal species at their active sites¹. In addition, the dioxygen molecule has been utilized as the cheapest abundant oxidant for organic oxidative transformations and most of the industrial processes are also realized by the action of transition metal catalysts². However, catalytic oxidation is far behind other catalytic reactions such as hydrogenation and polymerization. A key to development of new catalytic oxidative reactions may be obtained by analysis of the active centers of metalloproteins that participate in oxygenation and oxygen-transport. Analysis of the structure and the function of an active site followed by appropriate design of a catalyst system would lead to new catalytic processes.

In order to analyse the reaction mechanisms it is crucial to understand *how dioxygen and substrate molecules are incorporated and activated in the coordination environment created by the transition metal center*. In our laboratory, transition metal dioxygen complexes are studied from both organometallic and bioinorganic viewpoints.

2. Transition metal dioxygen complexes

A considerable number of transition metal dioxygen complexes have been reported so far³. Typical coordination structures are shown in figure 1. Most of them are mononuclear complexes characterized as the acyclic η^1 - or cyclic η^2 -structures (**I** and **II**, respectively, in

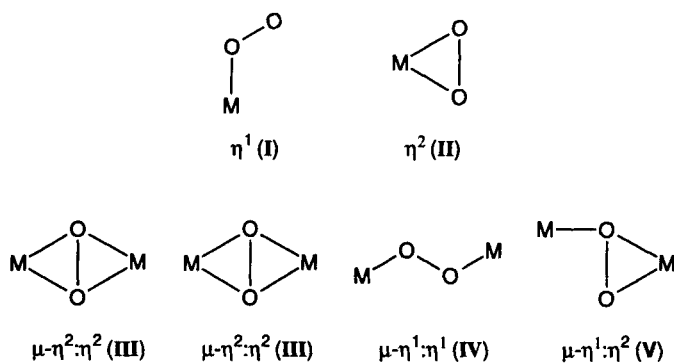


Figure 1. Typical interaction modes of O₂ with transition metal centers.

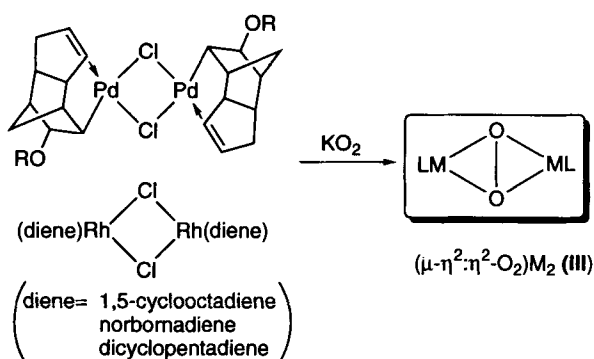
figure 1). However, they are not so reactive as had been expected and work as a simple base or a nucleophile rather than an electrophile. They can be simply added to an electron-deficient substrate to give oxidized products. For effective oxygenation of a substrate, conversion to an electrophilic oxygen species is essential. A typical activation method is the action of an electrophilic reagent (X) such as proton, acyl halide and an alkylating agent to induce formal, heterolytic O–O bond cleavage in the resulting M–O–O–X species. The resultant electrophilic oxene species (M=O) is reactive enough to functionalize aliphatic groups as typically exemplified by cytochrome P-450.

3. Dinuclear $\mu\text{-}\eta^2\text{:}\eta^2\text{-dioxo}$ complexes

Following the mononuclear dioxygen complex chemistry, the chemistry of the dinuclear version has been developed mainly in our laboratory^{4,5}. The first dinuclear $\mu\text{-}\eta^2\text{:}\eta^2\text{-dioxo}$ complexes of palladium and rhodium (type III) were prepared by metathesis reaction between transition metal halide and potassium superoxide (scheme 1)⁴. It is notable that the dioxygen complexes also contain potentially oxidizable substrate such as olefin and hydrocarbyl group as a ligand. As for their reactivity, however, remarkable oxidative transformation was not observed. The O₂ moiety worked as a base as observed for the mononuclear complexes, and stoichiometric O-atom transfer to the olefinic part is observed under forced conditions, although it was not selective.

Although the type III species of Pd and Rh turned out to be not so reactive as an intermediate of organic oxidative transformation, such a structure attracted renewed interest from bioinorganic viewpoints. Recently it has been revealed that many oxygenases and O₂-transport proteins contain a dinuclear metal center as the O₂-activation site. Hemocyanin (Cu₂), tyrosinase (Cu₂) and methanemonooxygenase (Fe₂) can be raised as typical examples and are also targets of bioinorganic studies including ours.

We succeeded in the synthesis and characterization of a variety of mono- and dinuclear dioxygen complexes by using bulky hydrotris(3,5-dialkylpyrazolyl)borate ligands (Tp^R: figure 2; in particular, the diisopropyl derivative, Tp^{iPr})^{5,6}. The Tp^R ligand is expected to mimic a coordination environment created by three facially arranged imidazolyl rings of His-residues and such a situation is frequently found in



Scheme 1.

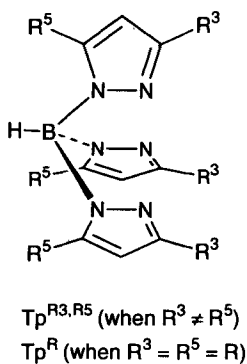
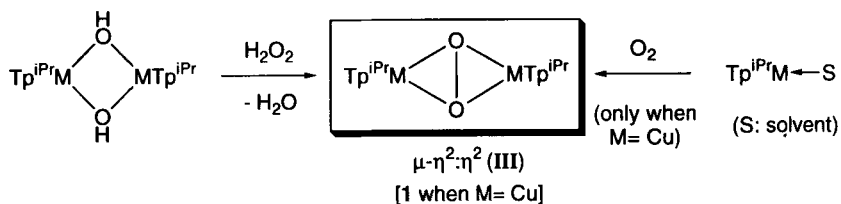


Figure 2. Hydrotris(pyrazolyl)borate ligands.

metalloproteins. Previous bioinorganic research work was focused on heme systems. $\text{M}-\text{O}_2$ species supported by a porphyrin ring shows characteristic spectroscopic features and does not allow extensive structural change. In contrast, non-heme metalloproteins are supported by a quite flexible protein chain, whose spectroscopic features are much less characteristic compared to heme-proteins.

The first successful application of the Tp^{R} ligand system was synthesis of a dicopper- O_2 complex^{6a}. It had been known that O_2 molecule was incorporated into the dicopper site in *hemocyanin* (O_2 -transport proteins of invertebrates). The structure of the O_2 -free species was determined by X-ray crystallography, which revealed that each of the two copper centers separated by 3.6 Å was coordinated by three histidyl residues. Thus this system was suitable for study using Tp^{R} ligands. A mountain of physicochemical data including O—O stretching vibration, UV-VIS spectra, and magnetism was also accumulated for the O_2 -bonded form (*oxyhemocyanin*). On the basis of the physicochemical data, various coordination models were proposed and corresponding model compounds (e.g. $\text{trans-}\mu-\eta^1:\eta^1$ -structure⁷; type IV in figure 1) were prepared. But

none of them could reproduce the physicochemical properties of *oxyhemocyanin*, in particular, the low O–O stretching vibration. Treatment of a solvent-stabilized $\text{Tp}^{\text{iPr}}\text{Cu}(\text{I})$ species [Tp^{iPr} : hydrotris(3,5-diisopropylpyrazolyl)borate] with O_2 gave a diamagnetic dicopper(II) species **1** (scheme 2). It was notable that physicochemical properties of the



Scheme 2.

dicopper complex **1** such as the Raman frequency of the O–O vibration, UV spectrum, and magnetism showed good agreement with those of *oxyhemocyanin* as compared in table 1. X-ray crystallographic analysis of **1** revealed the $\mu\text{-}\eta^2\text{:}\eta^2\text{-O}_2$ -coordination mode (III in figure 1), which we proposed as the most probable O_2 -coordination structure of *oxyhemocyanin*. Later *oxyhemocyanin* obtained from *Limulus polyphemus* was characterized by X-ray crystallography and it was revealed that dioxygen molecule was coordinated to the dicopper center in the $\mu\text{-}\eta^2\text{:}\eta^2$ -fashion as we predicted⁸.

Subsequently we developed an alternative widely applicable synthetic method of dioxygen complex, i.e. dehydrative condensation between a hydroxo complex and hydrogen peroxide (scheme 2). Related species such as hydro- and alkylperoxo complexes, $\text{Tp}^{\text{R}}\text{M}\text{-OOR}'$, were accessible via this method, i.e. $[\text{Tp}^{\text{R}}\text{M}(\text{OH})]_n + \text{R}'\text{OOH}$ ($\text{R}' = \text{alkyl, H}$)⁹.

As for the reactivity of **1**, the O_2 -moiety is still nucleophilic. Complex **1** can bind O_2 molecule without O–O bond cleavage. This behaviour well reproduces the role of the dicopper species as an O_2 -transport protein. It is also known that a similar $(\mu\text{-}\eta^2\text{:}\eta^2\text{-O}_2)\text{Cu}_2$ structure is involved in the active site of tyrosinase, an enzyme which converts phenol into

Table 1. Comparison of selected spectroscopic and structural parameters for $\mu\text{-}\eta^2\text{:}\eta^2\text{-O}_2$ dimetal species and related species

Compound	$\lambda_{\text{max}}/\text{nm}$ ($\epsilon/\text{M}^{-1} \text{cm}^{-1}$)	$\nu_{\text{O-O}}$ (cm^{-1})	O–O (Å)	Cu–Cu (Å)
$(\mu\text{-}\eta^2\text{:}\eta^2\text{-O}_2)(\text{CuTp}^{\text{iPr}})_2$ (1)	349 (21000), 551 (790)	741	1.41	3.56
$(\mu\text{-}\eta^2\text{:}\eta^2\text{-O}_2)(\text{CuTp}^{\text{Me}})_2$	338 (20800), 530 (840)	731		
$(\mu\text{-}\eta^2\text{:}\eta^2\text{-O}_2)(\text{CuTp}^{\text{Ph}})_2$	355 (18000), 542 (1040)	759		
<i>Oxyhemocyanin</i>	340 (20000), 580 (100)	744–752		3.5–3.7
<i>Oxytyrosinase</i>	345 (18000), 600 (1200)	755		~3.6
$(\mu\text{-}\eta^2\text{:}\eta^2\text{-O}_2)(\text{CuTp}^{\text{iPr}})_2$ (2)	350 (8900), 493 (2900)	651		
$(\mu\text{-O}_2)(\text{NiTp}^{\text{iPr}})_2$ (9)	304 (12000), 404 (10500)	<i>a</i>		
$(\mu\text{-}\eta^2\text{:}\eta^2\text{-O}_2)(\text{CuTACN}^{\text{iPr}_3})_2$ (13)	366 (22500), 510 (1300)	722		
$(\mu\text{-O}_2)(\text{CuTACN}^{\text{iPr}_3})_2$ (13')	324 (11000), 448 (13000)	<i>a</i>	2.97	2.79

^anot located.

o-quinone derivative. Complex **1** can also oxidize phenol derivatives to give diphenoquinone instead of *o*-quinone. Although the reaction mechanism is still in controversy, we have proposed a mechanism involving hydroperoxide (Cu–OOH) and phenolate intermediates (Cu–OAr) arising from protonolysis of the Cu₂(O₂) core with phenol. Attack of the hydroperoxide species to the phenolate species would result in oxidation at the *ortho*-position to give *o*-quinone¹⁰.

4. Conversion of (μ - η^2 : η^2 -O₂)M₂ species into bis(μ -oxo)dimetal species

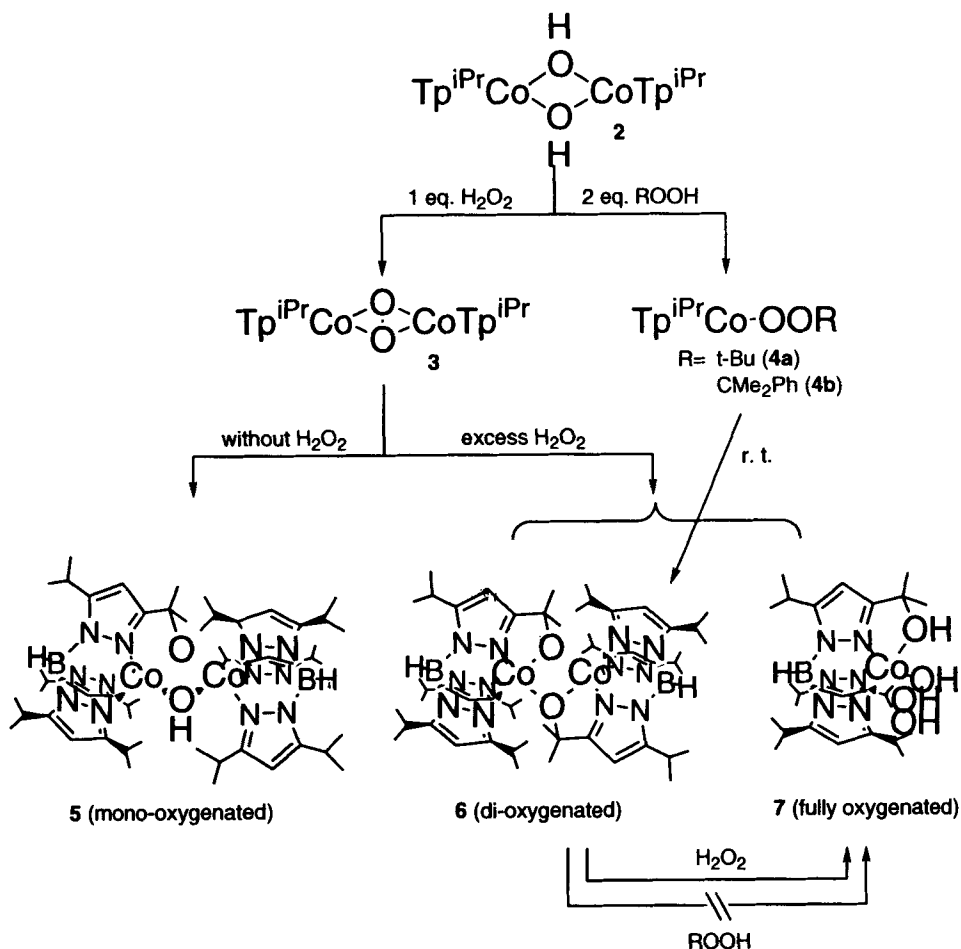
Following the study on the Cu complex, we now extend the study on Tp^RM–O₂ complexes to other metal species (Ni, Co, and the second row metals), which are not relevant to the biological systems. For comprehensive understanding of transition metal-dioxygen interaction, systematic synthesis and comparative study of LM–O₂ complexes supported by the same ligand (L) is crucial but such chemistry has not appeared so far. We have revealed that the Tp^R ligand is suitable for this purpose, because (i) it gives divalent species irrespective of the central metal and (ii) the precursors, hydroxo complexes, are available by hydrolysis of the corresponding halo and carboxylato complexes. Application of the dehydrative condensation method of O₂-complexes (scheme 2) to Co and Ni systems results in the successful generation of the type III(μ - η^2 : η^2 -O₂)M₂ species. Their reactivity and structure, however, are considerably different from those of the Cu complex as described below.

4.1 Cobalt peroxo complexes^{11,12}

Cobalt is the most studied element of the synthetic metal–dioxygen complexes. Previous studies have revealed that the typical oxidation state of the metal center in the Co peroxo complexes is Co(III). In fact, many Co(III) peroxo complexes have been isolated, but only a limited number of Co(II) dioxygen complexes such as mono- and dinuclear superoxo complexes and μ -peroxo complex have been characterized. At first, we attempted oxygenation of the dinuclear Co(II) bis(μ -hydroxo) complex, [Tp^{iPr}Co(μ -OH)]₂ (**2**)¹³. However, **2** was found to be unreactive toward dioxygen and never gave Co(III) compounds. Then **2** was subjected to reaction with H₂O₂ (scheme 3).

Reaction of the bis(μ -hydroxo) complex **2** with an equimolar amount of H₂O₂ at –50°C afforded a dark brown compound **3**, which could not be fully characterized due to its thermal instability. The reaction product **3** can be identified as either of a dinuclear Co(II) μ - η^2 : η^2 -peroxo complex, [Tp^{iPr}Co]₂(μ -O₂)¹¹, or a bis(μ -oxo) complex, [Tp^{iPr}Co]₂(μ -O)₂, resulting from O–O bond cleavage. The UV-VIS spectrum of **3** (λ_{max} : 350 and 493 nm) is similar to that of **1** (λ_{max} : 349 and 551 nm) but the O–O stretching vibration of **3** (651 cm^{–1}; Raman) appears far below that of **1** (741 cm^{–1}). The notable red-shift of the O–O stretching vibration is presumably attributed to the increased back-donation from the metal center to the vacant O–O orbital of antibonding character, because the d-orbital levels of Co are higher than those of Cu. This indicates that the O–O bond in the Co complex **3** is considerably weakened compared to that in the Cu complex **1**, and the different reactivity of **1** and **3** (see below) should reflect the electronic state of their O₂ moieties.

As a comparative study, synthesis of alkylperoxo complex was also examined. Treatment of a pentane solution of the hydroxo complex **2** with 2 equivalents of alkyl hydroperoxide at –78°C gave a blue solution with an intense absorption around 650 nm



Scheme 3.

(scheme 3), that was characteristic of a high-spin Co(II) ion located in a tetrahedral ligand field. Although the isolation of the thermally unstable **4** was also unsuccessful, it was identified as a tetrahedral Co(II) alkylperoxo compound, $\text{Tp}^{\text{iPr}}\text{Co}(\text{OOR})$ [$\text{R} = t\text{-Bu}$ (**4a**), CMe_2Ph (**4b**)], by comparison with the structurally characterized $\text{Tp}^{\text{Bu},\text{Pr}}\text{Co}(\text{OOCMe}_2\text{Ph})$ (**4c**), which was stabilized by a more hindered hydrotris(3-*tert*-butyl-5-isopropyl-1-pyrazolyl)borate ligand ($\text{Tp}^{\text{Bu},\text{Pr}}$).

The Co(II)-peroxo complexes **3** and **4** were thermally unstable compared to the copper complexes. Spontaneous decomposition of these Co(II) peroxo species resulted in the oxygenation of the isopropyl substituents attached to the pyrazolyl ligands and the different decomposition products were obtained from **3** depending on the conditions (absence or presence of H_2O_2) (scheme 3).

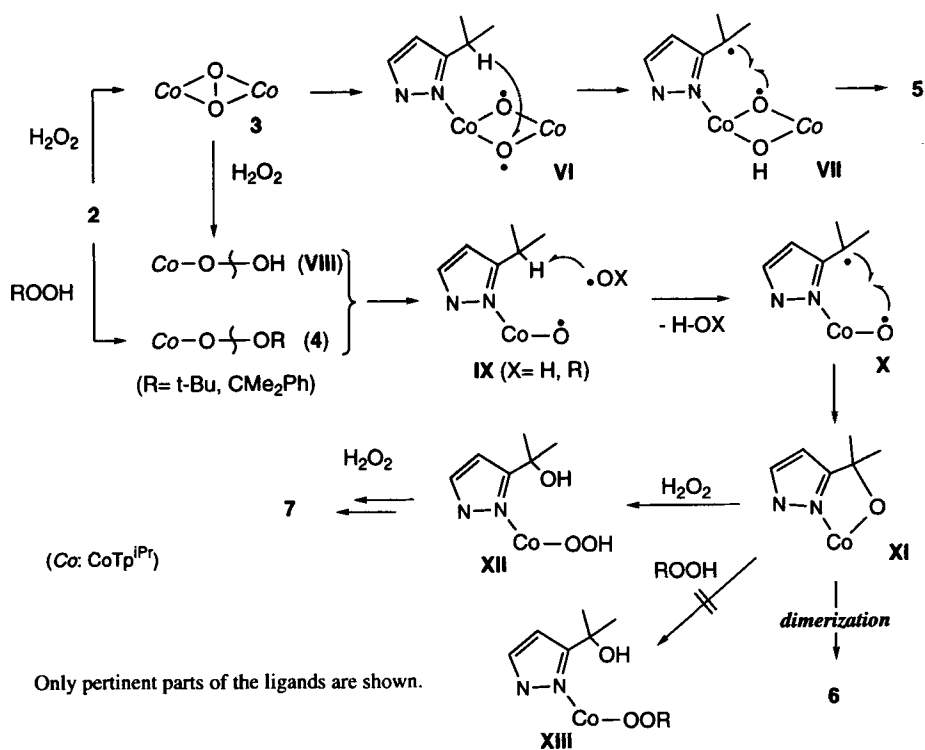
The decomposition of **3** at ambient temperature in the absence of H_2O_2 produced mono-oxygenated compound **5**, which was characterized by X-ray crystallography as a μ -alkoxo- μ -hydroxo dinuclear Co(II) complex. It is notable that *one* of the six methine

groups in the isopropyl substituents proximal to the metal centers in **3** is oxygenated and the resulting alkoxide functional group bridges the two Co(II) centers.

On the other hand, decomposition of **3** at room temperature in the presence of an excess amount of H_2O_2 resulted in the formation of a mixture of two further oxygenated products. When 10 equivalents of aqueous H_2O_2 were added to a toluene solution of **2** at -78°C , the red solution changed to a dark brown one, indicating the formation of the μ -peroxo complex **3**. After the resulting mixture was warmed to room temperature without removal of the excess H_2O_2 and then stirred for 12 h, the deep blue-green crystals **6** and the pale brown crystals **7** were isolated by fractional crystallization and characterized successfully by X-ray crystallography. In the dinuclear compound **6** two of the six proximal isopropyl methine carbon atoms in **3** are oxygenated, and the resultant chelating alkoxide ligands bridge the two Co(II) ions to give the symmetrical, dimeric structure. In contrast to the structures of **5** and **6**, the pale brown product **7** is the *mononuclear* Co(II) hydroxo alcohol complex and its most striking structural feature is that all *three* methine sites of the proximal Pr^i groups are fully oxygenated.

Alkylperoxo complexes **4** also decomposed to give the di-oxygenated, *bis*(μ -alkoxo) compound **6**. However, it is noteworthy that the fully oxygenated compound **7** was not formed even in the presence of a large excess amount of ROOH. Reaction of **6** with ROOH also did not form **7**, whereas reaction with H_2O_2 gave **7**.

Plausible reaction mechanisms for the Co system are summarized in scheme 4. Formation of the mono-oxygenated product **5** from **3** can be explained in terms of the



Scheme 4.

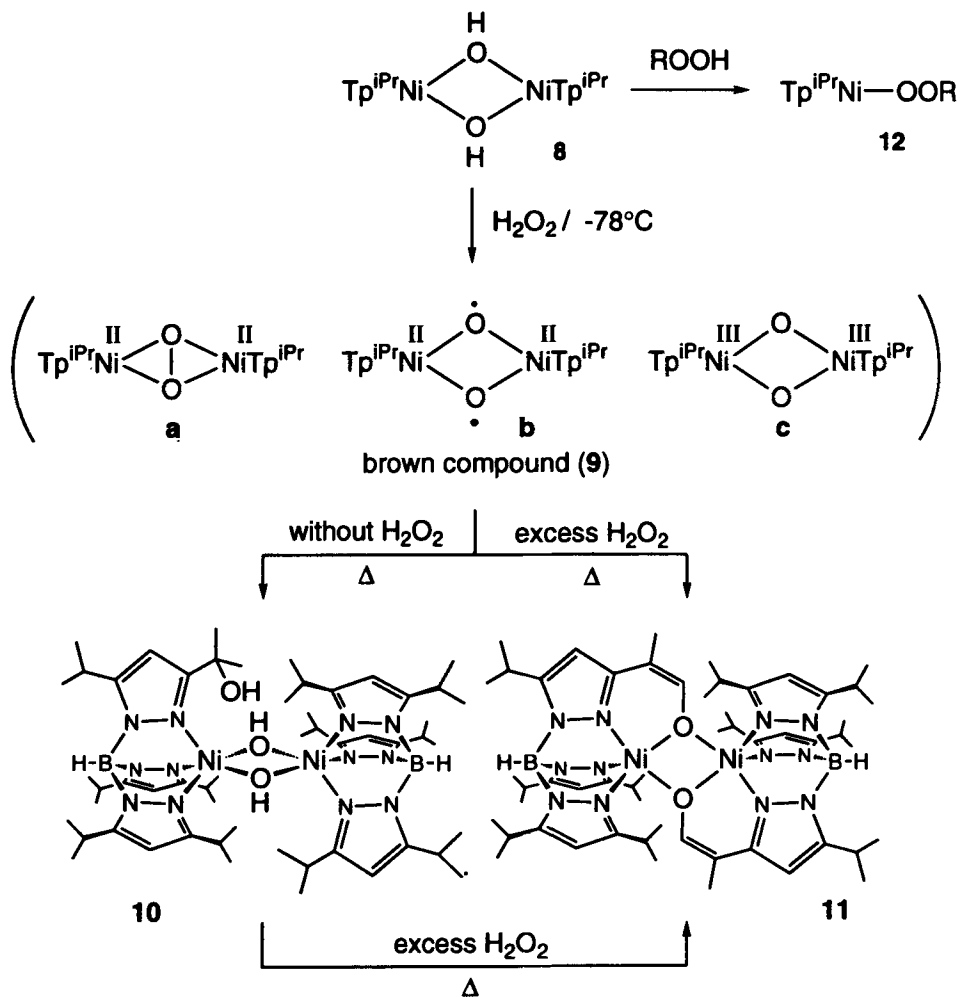
following reaction sequence: (i) Homolysis of the O–O bond, (ii) abstraction of a proximal isopropyl methine hydrogen atom by one of the two resulting oxyl radicals (VI), and (iii) coupling between the formed tertiary radical and the remaining oxyl radical (VII). Other mechanisms such as concerted C–H breaking associated with the subsequent C–O bond formation are also possible. In the case of the decomposition of **3** in the presence of excess H₂O₂, protonolysis of the Co–O part with H₂O₂ forms two equivalents of the mononuclear hydroperoxo species VIII. Subsequent radical processes, analogous to those mentioned above, give a chelating alkoxo intermediate IX, dimerization of which gives a di-oxygenated product **6**. But a part of XI may further react with excess H₂O₂ to produce another hydroperoxo intermediate XII. Repetition of the oxygenation processes analogous to VIII(XII) → IX → X → XI → XII finally leads to the formation of the fully oxygenated product **7**. The thermal degradation of the alkylperoxo species **4** should follow a similar reaction sequence as mentioned above to give the di-oxygenated, dinuclear complex **6**. However, in this case, alkyl hydroperoxide is not acidic enough to hydrolyze the chelating alkoxo intermediate XI, because the alkyl substituent, which is more electron-donating than the hydrogen atom, reduces the acidity of the OOH part. Therefore formation of the next alkylperoxo intermediate XIII is unfavourable. The reaction stops at the stage of XI and then goes to **6**.

4.2 Nickel peroxo complexes¹⁴

The dehydrative condensation method (scheme 2) is also effective for the Ni system. Treatment of the dinuclear Ni(II) *bis*(μ-hydroxo) complex **8**¹³ with H₂O₂ at –78°C gave an extremely thermally unstable dark brown compound **9** (scheme 5). In an absorption spectral titration experiment of **8** (an ethereal solution) with H₂O₂, the intensity of the absorptions at 304 and 404 nm due to **9** reach the maximum, when the **8** : H₂O₂ ratio is unity, and no further change is observed on addition of an excess amount of H₂O₂. The presence of two Ni(II) centers antiferromagnetically coupled through the bridging ligands is suggested by its ¹H-NMR resonances appearing in the range of 1–8.5 ppm. The spectrum is in sharp contrast to the paramagnetically shifted spectrum of **8**. These spectroscopic characteristics are consistent with a μ-peroxo dinickel(II) structure (**9a**) as observed for the μ-η²:η²-peroxo Cu and Co complexes or di-μ-oxyl dinickel(II) species (**9b**) [or a di-μ-oxo dinickel(III) species (**9c**)] resulting from O–O bond homolysis of the peroxo ligand. Although the measurement of the O–O vibration was attempted in order to determine the O–O bond order, it was unsuccessful due to its thermal instability. The dark brown intermediate **9** has been tentatively assigned to either of the latter two structures (**9b** or **9c**), because the following reaction study indicates its radical character.

Complex **9** decomposed spontaneously within a minute even at –50°C to give a ligand-hydroxylated compound **10**, which was characterized by X-ray crystallography. The formulation is also supported by the molecular ion peak corresponding to a μ-carbonato complex, T^p^{iPr}Ni(μ-CO₃)Ni[HB(3-Me₂C(OH)-5-Prⁱpz)(3,5-Prⁱpz)₂] (**10** + CO₂ – H₂O). (We reported that dinuclear *bis*(μ-hydroxo) complexes like **10** were so sensitive to CO₂ in the air as to form μ-carbonato complexes¹³.)

Interestingly, treatment of **8** with an excess amount of H₂O₂ brought about concomitant oxygenation and dehydrogenation of the Prⁱ groups to give the enolato complex **11**. Its IR spectrum contains strong absorptions at 1616 cm^{–1} and 1203 cm^{–1} which were assigned as the C=C and C–O vibrations, respectively, and its structure was definitely confirmed by X-ray crystallography.



Scheme 5.

The hydroxo complex **8** also reacted with ROOH to give the alkylperoxy complex **12**, the $\text{Tp}^{\text{Bu},\text{Pr}}$ derivative of which was characterized crystallographically¹⁴. Thermal decomposition of **12** did not afford either **10** or **11** but ligand hydroxylation appeared to occur as judged by a ¹H-NMR spectrum. Details remain to be studied.

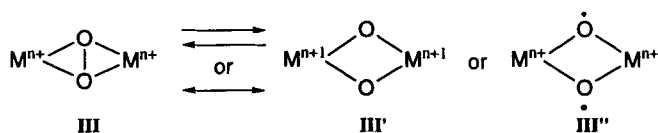
The alkane functionalization observed for the present Ni system is slightly different from that observed for the cobalt system (scheme 3). We propose two reaction mechanisms for the conversion of **8** to **10**. One mechanism is similar to that of the cobalt system (scheme 4); a proximal methine hydrogen atom is abstracted by the oxyl species in **9b** (cf. VI), then the resulting alkyl radical couples with the remaining Ni-O[•] to afford **10** after hydrolysis of the chelating alkoxy moiety. Another possible mechanism involves the dinuclear Ni(III)-bis(μ -oxo) intermediate **9c**. The proximal H atom is abstracted by the Ni-oxo species, and “rebound” between the resulting tertiary alkyl radical and the OH radical followed by hydrolysis furnishes the final product **10**. However, because the two structures **9b** and **9c** can be recognized as two extremes of canonical formulation, the two mechanisms are not so different.

Reaction with an excess amount of H_2O_2 results in the formation of an enolato complex **11** instead of further oxygenated complexes like **6** and **7** arising from the mononuclear $\text{M}-\text{OOH}$ species. The formation of **11** by treatment of an isolated sample of **10** with H_2O_2 suggests that **10** is its intermediate. It is notable that treatment of **3** with ROOH ($\text{R} = t\text{-Bu}$, PhMe_2C) does not yield **11**. These observations suggest that a dinuclear intermediate such as $[\text{Ni}(\text{III})-(\mu\text{-O})_2]$, $\text{Ni}(\text{II})-(\mu\text{-}\eta^2\text{:}\eta^2\text{-O}_2^{2-})\text{-Ni}(\text{II})$, and $[\text{Ni}(\text{II})\text{-OOH}]_2$ species, not a mononuclear one, may be involved in the present functionalization process.

5. Conclusion

Cu (**1**), Co (**3**) and Ni (**9**) peroxo complexes of type **III** are generated by the dehydrative condensation method (scheme 2). In contrast to the Cu complex **1**, the $\text{O}-\text{O}$ bond in **3** and **9** is readily cleaved in a homolytic fashion to form the oxyl radical intermediate (**IV** and **9b**) [or di- μ -oxo-species of higher oxidation state **9c**], which causes functionalization ($\text{C}-\text{H}$ activation) of the proximal isopropyl group to give the oxygenated products **5**, **6**, and **10**. Quite recently we succeeded in isolation and structural characterization of the $\text{O}-\text{O}$ cleaved form of related species. In addition, the present study reveals that transition metal hydroperoxo and alkylperoxo intermediates serve as active species of $\text{C}-\text{H}$ bond oxygenation.

Recently, Tolman *et al*¹⁵ reported equilibrium between the $(\mu\text{-}\eta^2\text{:}\eta^2\text{-O}_2)\text{M}_2$ structure **III** and the higher valent *bis*(μ -oxo) structure **III'** [or the *bis*(μ -oxyl radical) structure **III''**] for the copper-dioxygen complex **13** supported by substituted 1,4,7-triazacyclononane (TACN) ligands, N_3 -ligands similar to Tp^{R} (table 1)¹⁵. Combined with



Scheme 6.

our result, these observations led to an idea of new activation mode of dioxygen molecule: $\mu\text{-}\eta^2\text{:}\eta^2\text{-Perox}$ species has the potential to exhibit high oxidizing power via homolytic $\text{O}-\text{O}$ bond scission. The high reactivity of the $\text{M}(\mu\text{-O})_2\text{M}$ core should be ascribed to its electrophilic nature typically expressed by the higher oxidation state form **III'**, and the $[\text{M}-\text{O}]_n$ system of high oxidation state would work as an efficient oxidizing agent like electrophilic oxene species ($\text{M}=\text{O}$). Before closing this part, let us point out the relationship between the reactivity of dioxygen complexes and $\text{O}-\text{O}$ stretching vibration. This is a view of the electronic state of the $\text{O}-\text{O}$ moiety. As mentioned in the introductory part, mononuclear complexes were the previous major research target. $\nu(\text{O}-\text{O})$ values of mononuclear complexes **II** ($> 800 \text{ cm}^{-1}$) indicate multiple bond character of the $\text{O}-\text{O}$ moiety and, actually, they only show nucleophilic reactivity. No dioxygen complex showing $\nu(\text{O}-\text{O})$ band lower than 800 cm^{-1} was known until we reported the type **III** dinuclear complexes (figure 3). Upon the complexation to the second metal center, the $\nu(\text{O}-\text{O})$ band shifts to lower energies as observed for the dicopper complex **1** (741 cm^{-1}). The $\nu(\text{O}-\text{O})$ value suggests that the $\text{O}-\text{O}$ bond order is considerably reduced as compared with organic peroxide [$\text{R}-\text{O}-\text{O}-\text{R}$: ($890\text{--}830 \text{ cm}^{-1}$)] but the electron transfer to the antibonding $\text{O}-\text{O}$ σ^* orbital, which weakens the $\text{O}-\text{O}$ bond, is still insufficient for $\text{O}-\text{O}$

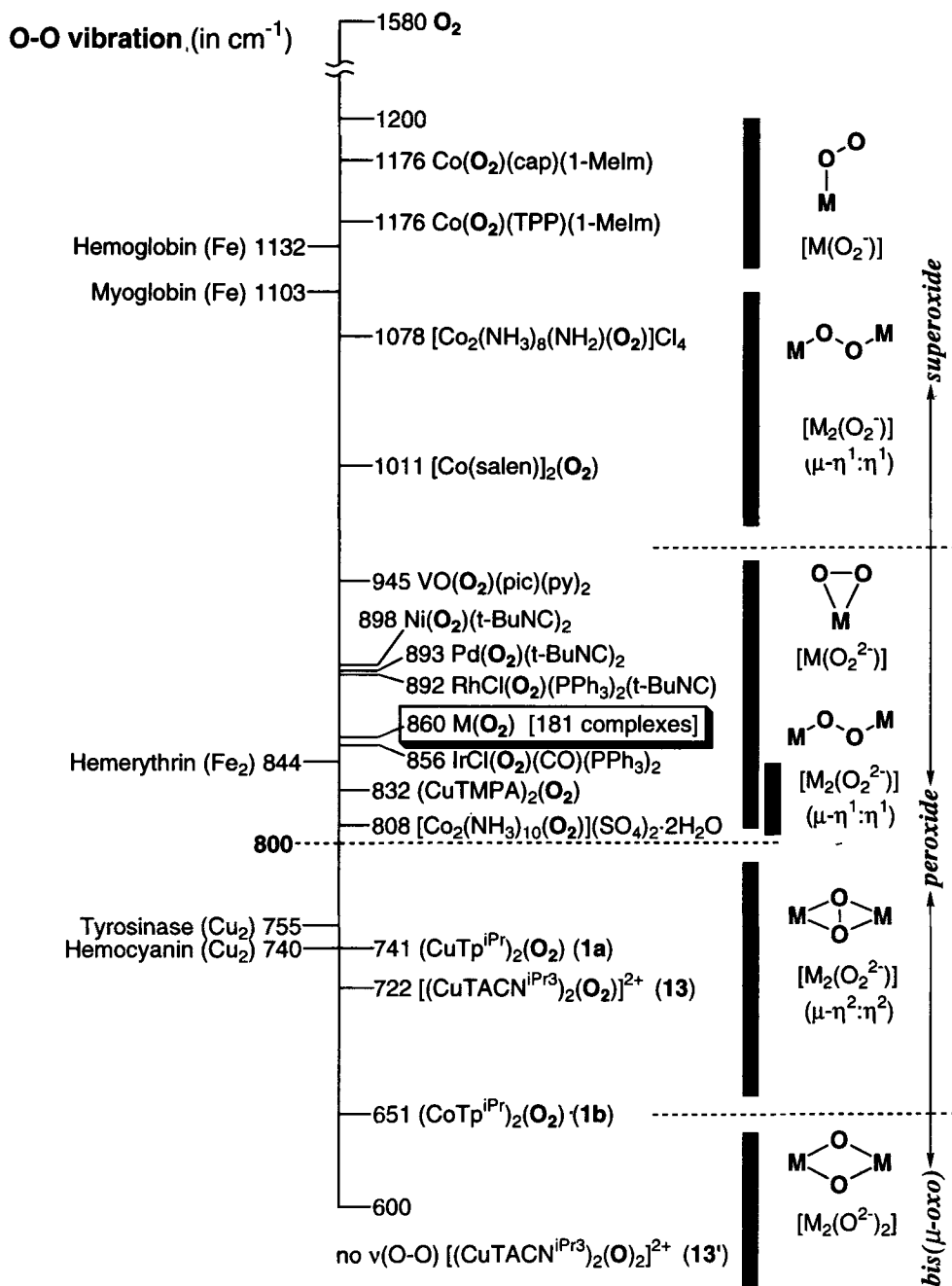


Figure 3. Comparison of $\nu(\text{O-O})$ values and coordination structures of transition metal-dioxygen complexes.

bond breaking. Finally, the introduction of more electron-donating elements (Co, Ni) or more electron-donating ligands such as TACN causes scission of the O–O bond, when the $\nu(\text{O-O})$ band is much lower ($722\text{--}657\text{ cm}^{-1}$), and high reactivity is realized.

Thus the stability of the $(\mu\text{-}\eta^2\text{-}\eta^2\text{-O}_2)\text{M}_2$ complexes **1**, **3**, and **9** depends on the electron-donating ability of the central metal atom, and the difference arises mainly from the extent of back-donation to the antibonding O–O orbital. Although their relative stability [**1**(Cu) > **3**(Co) > **9**(Ni)] does not always correspond to the d-orbital levels (Co > Ni > Cu), the opposite order between Co and Ni may be explained in terms of the different coordination geometries that they favour. Further studies on various chemical and biological oxidation systems may reveal participation of **III–III'** type intermediates as a key intermediate in oxidative transformations. Although only intramolecular oxidation is observed for the $\text{Tp}^R\text{M–O}_2$ systems at the moment, study aiming for oxidation of external substrates is now underway and new catalytic reactions involving the **III** → **III'** (or **III''**) process as a key step will be developed in the future.

References

1. (a) The thematic issue of *Chem. Rev.* (metal dioxygen complexes), *Chem. Rev.* 1994 **94** 567–856 (b) the thematic issue of *Chem. Rev.* (bioinorganic enzymology), *Chem. Rev.* 1996 **96** 2239–3042
2. (a) Sheldon R A and Kochi J K 1981 In *Metal-catalyzed oxidation of organic compounds* (New York: Academic Press) (b) Mukaiyama T and Yamada T 1995 *Bull. Chem. Soc. Jpn.* **68** 17
3. (a) Lyons J A 1977 *Aspects Homog. Catal.* **3** 1 (b) Gubelmann M H and Williams A F 1983 *Struct. Bonding* **55** 1 (c) Kitajima N, Akita M and Moro-oka Y 1992 In *Organic peroxides* (ed.) W Ando (New York: Wiley) pp 535–558
4. (a) Suzuki H, Mizutani K, Moro-oka Y and Ikawa T 1979 *J. Am. Chem. Soc.* **101** 748 (b) Chung P J, Suzuki H, Moro-oka Y and Ikawa T 1980 *Chem. Lett.* 63 (c) Sakurai F, Suzuki H, Moro-oka Y and Ikawa T 1980 *J. Am. Chem. Soc.* **102** 1749 (d) Sugimoto R, Suzuki H, Moro-oka Y and Ikawa T 1982 *Chem. Lett.* 1863
5. Kitajima N and Moro-oka Y 1994 *Chem. Rev.* **94** 737
6. (a) Kitajima N, Fujisawa K, Fujimoto C, Moro-oka Y, Hashimoto S, Kitagawa T, Toriumi K, Tatsumi K and Nakamura A 1992 *J. Am. Chem. Soc.* **114** 1277 (b) Kitajima N, Tamura N, Amagai H, Fukui, H, Moro-oka Y, Mizutani Y, Kitagawa T, Mathur R, Heerwegh K, Reed C A, Randall C R, Due L Jr and Tatsumi K 1994 *J. Am. Chem. Soc.* **116** 9071 (c) Kitajima N, Osawa M, Tanaka M and Moro-oka Y 1991 *J. Am. Chem. Soc.* **113** 8952 (d) Kitajima N, Komatsuzaki H, Hikichi S, Osawa M and Moro-oka Y 1994 *J. Am. Chem. Soc.* **116** 11596
7. (a) Karlin K D, Cruse R W, Gultneh Y, Hayes J C and Zubieta J 1984 *J. Am. Chem. Soc.* **106** 3372 (b) Karlin K D, Cruse R W, Gultneh Y, Farooq A, Hayes J C and Zubieta 1987 *J. Am. Chem. Soc.* **109** 2668
8. (a) Magnus K A, Hazes B, Ton-That H, Bonaveture C, Bonaveture J, Hol W G J 1994 *Proteins* **19** 302 (b) Magnus K A, Ton-That H and Carpenter J E 1994 *Chem. Rev.* **94** 727
9. Kitajima N, Katayama T, Fujisawa K, Iwata Y and Moro-oka Y 1993 *J. Am. Chem. Soc.* **115** 7872
10. Kitajima N, Koda T, Iwata Y and Moro-oka Y 1990 *J. Am. Chem. Soc.* **112** 8833
11. Hikichi S, Komatsuzaki H, Kitajima N, Akita M, Mukai M, Kitagawa T and Moro-oka Y 1997 *Inorg. Chem.* **36** 266
12. Hikichi S, Komatsuzaki H, Akita M and Moro-oka Y 1998 *J. Am. Chem. Soc.* **120** 4699
13. Kitajima N, Hikichi S, Tanaka M and Moro-oka Y 1993 *J. Am. Chem. Soc.* **115** 5496
14. Hikichi S, Yoshizawa M, Sasakura Y, Akita M and Moro-oka Y 1998 *J. Am. Chem. Soc.* **120** 10567
15. (a) Halfen J A, Mahapatra A, Wilkinson E C, Kaderli S, Young V G Jr, Que L Jr, Zuberbühler A D and Tolman W B 1996 *Science* **271** 1397 (b) Mahapatra A, Halfen J A, Wilkinson E C, Pan G, Wang X, Young V G Jr, Cramer C J, Que L Jr and Tolman W B 1996 *J. Am. Chem. Soc.* **118** 11555 (c) Tolman W B 1997 *Acc. Chem. Res.* **30** 227